

Scattering Patterns of Multiply Continuous Cubic Phases in Block Copolymers. II. Application to Various Triply Periodic Architectures

Piotr Garstecki^{†,‡} and Robert Holyst^{*,†,§}

Institute of Physical Chemistry PAS Department III, Kasprzaka 44/52, 01-224 Warsaw, Poland, and Cardinal Stefan Wyszyński University, WMP–SNS, Dewajtis 5, Warsaw, Poland

Received August 5, 2002; Revised Manuscript Received August 8, 2003

ABSTRACT: The model for the scattering amplitudes is applied to a quantitative analysis of the scattering spectra of the *n*-block copolymer systems. The method allows interpretation of the X-ray diffraction patterns in systems of the multiblock copolymers forming multiply continuous triply periodic structures (MCTPS). We give simple formulas for the scattering intensity for structures of different topology and symmetry appearing in block copolymers. The straightforward fitting procedure presented in this article allows determination of the multicontinuous architecture adopted by a multiblock copolymer system, the volume fractions of the continuous domains and the width of the interdomain interfaces. The model is robust, i.e., applicable to *n*-block linear copolymers, and should be helpful in the quantitative analysis of the experimental data.

1. Introduction

The first report on the existence of cubic continuous phases in block copolymer mixtures dates back to 1986.¹ Since then a number of experimental studies^{2–9} have been devoted to these systems. The multicontinuous polymer network materials can have a large number of applications ranging from photonic band gap materials^{10,11} to ceramic nano-objects¹² of interesting mechanical properties.

The most commonly observed cubic phase in the block copolymer blends is the tricontinuous gyroid (G) structure^{13–16} phase with five distinct continuous regions. It has also been identified¹⁷ in a PI–PS–PDMS system. Also the plumber's nightmare P structure has been reported experimentally.^{12,18} Theoretically the D – double diamond structure has been predicted in gyroid–diamond¹⁹ and gyroid–diamond–plumber's nightmare²⁰ phase sequences resembling surfactant systems. The theoretical modeling of the multiply continuous interfaces in block copolymer systems provides a rich variety of structures.²¹ Theoretical works show that there are gyroid structures far more complicated than the simple G structure.²² The determination of the structure still presents a major problem. It is enough to recall the confusion in the identification analysis between the double diamond structure¹ and bicontinuous gyroid^{14,23} in the polystyrene–polyisoprene diblock systems and between the OTDD²⁴ (ordered tricontinuous double diamond) and tricontinuous gyroid^{16,25} structures in the isoprene–styrene–2-vinylpyridine triblock systems. The number of possible structures grows exponentially with the number of different blocks in block copolymers,^{26–28} and thus the block copolymer systems still hold a promise for new, previously unexplored multicontinuous cubic phases.

The model which we have described in our preceding²⁹ article will be applied to various cubic block copolymer

architectures. The influence of the structure, the number, volume fractions and interface widths of the continuous channels on the small-angle X-ray scattering (SAXS) patterns will be investigated. This paper is meant to provide a general insight into possible cubic architectures formed in block copolymer systems and describe in detail the methods of a quantitative analysis of their SAXS spectra. Despite a rich history of both experimental and theoretical studies of the cubic phases formed in block copolymer mixtures there are no simple theoretical tools which can be easily³⁰ applied to the analysis of the X-ray scattering intensities. The method presented below is similar to the one which we have successfully applied to the analysis of the surfactant–water systems, where complex continuous structures are formed with channels of water interwoven with channels formed by surfactant bilayer.^{31,32} The main difference between both systems comes from the fact that structures formed in water–surfactant systems are symmetric with respect to the base minimal surface while those in block copolymers can be asymmetric. This results in different formulas for the scattering intensities. The structures formed in low-molecular weight surfactant systems are almost always the symmetric, three channel structures of the ABA type (water–surfactant–water), whereas the block copolymers can form either symmetric or asymmetric structures with, at least theoretically, arbitrarily large number of continuous channels.

We will give straightforward examples of application of our model²⁹ for the analysis of the experimental spectra. Given the basic knowledge of the composition of the system, simple assumptions of the possible architectures can be directly verified. This in turn should lead to a facilitated determination of the structure of the cubic phase found in the given block copolymer system.

The next section provides general remarks concerning the X-ray or neutron scattering techniques. Sections 3 and 4 discuss the various multi continuous architectures which can be found in di- and triblock copolymer system respectively and a detailed description on how to construct the scattering patterns. Section 5 describes a

[†] Institute of Physical Chemistry PAS Department III.

[‡] Present address: Chemistry & Chemical Biology Department, Harvard University, 12 Oxford St., Cambridge, MA 02138. E-mail: pgarstecki@gmwgroup.harvard.edu.

[§] Cardinal Stefan Wyszyński University.

method for extracting the interface width between the continuous domains from SAXS spectra.

2. Extracting the Experimental Intensity

The scattering experiments on block copolymer systems can be done either with the X-ray apparatus or with the neutron beams in a synchrotron. Although we are using the nomenclature of the small-angle X-ray scattering, the methods presented below can be also applied to the neutron scattering data. To do so, one only needs to substitute the electron densities of the blocks by the nuclei scattering length density. The most important difference between different experimental setups is the kind of the detector used. In any case either for one- or two-dimensional detector one can recover the original scattering intensity by using the appropriate Lorentz-polarization factors.³² When we refer to the experimental intensities, we assume that such corrections have already been applied.

Another important feature is the polycrystallinity of the sample. In the case of the cubic phases in lyotropic liquid crystals the long-range order is most often difficult to obtain. However, to our knowledge, most of the block copolymer cubic samples are highly textured and exhibit long-range order with large monocrystalline domains. On one hand, it facilitates the analysis of the scattering spectra since one has a chance to measure all of the reflections independently. On the other hand, when the number of domains is on the order of 10 the peaks tend to merge, and resolving the intensities is difficult. Since the methods for such analysis strongly depend on the geometry of the sample and the orientations of the domains, we do not provide a general solution to this problem. An example of such an analysis can be found in ref 16, for example. A detailed review of the scattering techniques used for the structure characterization of polymer systems can be found in ref 33.

3. Diblock Systems

The structure of linear diblock copolymer molecule is defined by the chemistry of the constituting blocks A and B and the degree of polymerization N_A and N_B . From this we can calculate the volume fractions ϕ_A of monomers A and B (ϕ_B) in the system:

$$\phi_{A/B} = \frac{N_{A/B} V_{A/B}}{N_A V_A + N_B V_B} \quad (1)$$

where $V_{A/B}$ are the volumes occupied by single monomers of type A or B. The volume fractions of the blocks determine in turn the volume fractions of the A- and B-rich domains forming the ordered structures. This second relation depends on the architecture adopted by the system. If the AB diblock system exhibits a cubic symmetry and the volume fractions of A and B suggest a continuous structure, there still are four³⁴ possible realizations of the multiply continuous triply periodic structures. The simplest possibility is that there is only one interface surface parallel to the base TPMS. Such a surface divides the volume of the unit cell into two networks of channels. One of them contains A-type monomers while the B-type monomers are centered in the second network (AB Figure 3). In the case of unbalanced prototype TPMS interchanging the channels is not a symmetry operation. Thus, the two networks are not equivalent, and one should take into account

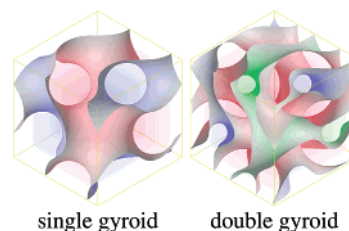


Figure 1. Left: Unit cells of the gyroid TPMS (left) dividing the volume into two distinct channels (red and blue). Right: Unit cell with two parallel surfaces derived from a gyroid TPMS. The three distinct subvolumes are marked with blue, red, and green.

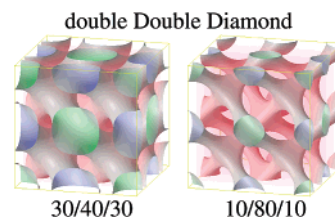


Figure 2. Unit cells of two parallel surfaces derived from a D-double diamond TPMS. Such surfaces divide the volume into three distinct but continuous subvolumes. In the first case (left) the volume fractions of the networks are 0.3, 0.4, and 0.3—blue, red, and green respectively. An analogous picture for 0.1, 0.8, and 0.1 fractions is shown in the right panel. Please note that provided the blue and green channels are filled with the same polymer species, and both the structure on the left and on the right are symmetric in respect to the base minimal surface. In general, in block copolymer systems, the green and blue channels need not have the same composition or size.

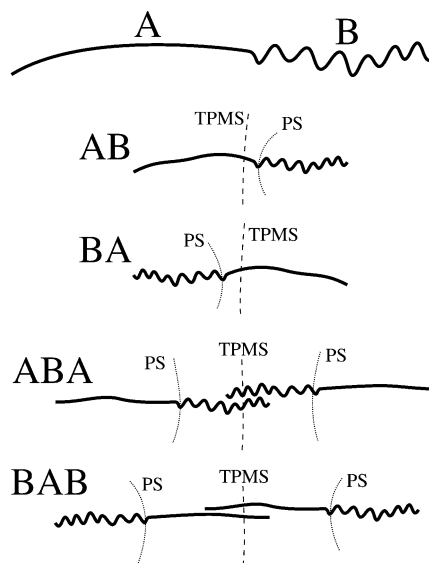


Figure 3. Schematic illustration of the possible multiply continuous cubic architectures formed in an AB diblock copolymer system. The base minimal surface (TPMS) divides the volume into two channels. If we name one *black* and the other *white* then the A blocks can occupy either a black side of the base TPMS (AB architecture) or an inverse situation is possible (BA). The two cases can be distinguished in the phases adopting a geometry given by an unbalanced TPMS. The two bottom sketches illustrate symmetrized architectures in which the unit cell is divided into three subvolumes. Then the A blocks can either occupy the two outermost channels (ABA architecture) or be centered within the layer separating them (BAB) architecture.

also an inverse possibility—namely the B blocks in the first channel and A in the second (BA Figure 3). The system might also tend to a higher symmetry which can be obtained by forming a structure with two interfaces.

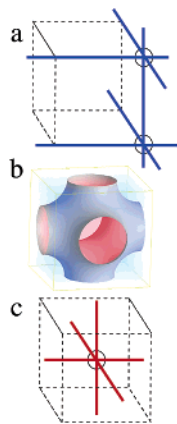


Figure 4. Unit cell of the P—plumber's nightmare TPMS is shown in part b. The upper and lower sketches show the connectivity of the two identical networks into which P TPMS divides the volume occupied by a monocrystalline domain.

The first one would have the A blocks in the two networks which are separated by a layer occupied by the B monomers. We will call this structure an ABA cubic system (ABA Figure 3). Finally the last possibility is a BAB structure.

In the case of the balanced prototypes, the choice between AB and ABA or BAB structures can be made upon the symmetry of the system. It comes from the fact that the ABA and BAB architectures are symmetric with respect to the base TPMS and belong to the same symmetry group. This is not true for the AB structure. In the case of the unbalanced base TPMS such a distinction is not possible because ABA structure belongs to the same symmetry group as AB. Furthermore, the structure factors (SF) and molecular factors (MF) can make some of the reflections very weak, which makes the determination of the symmetry by the analysis of the q spacings less reliable. An optimal procedure would consist of a quantitative analysis of the scattering intensities. To determine which structure has been formed in the system one should compare the experimentally measured intensities $\{I_i^{\text{exp}}\}$ of k peaks positioned at $\{q_i\}$ with the computed modeled intensities $\{I_i^{\text{type}}\}$. The best agreement points out to the most probable architecture of the system. We will show below that using the model derived in the preceding article makes such an analysis no longer computationally demanding.

3.1. Balanced Prototypes. Out of the four (P, D, G, and I-WP) TPMS discussed in this series of papers three are balanced (P, D, and G). Each one of them divides the volume into two identical systems of channels. Each system (network) is composed of cylinders joined at different coordination number characteristic for given TPMS (three for gyroid, four for double diamond and six for the plumber's nightmare). A schematic representation of the networks can be obtained by drawing straight lines between the nodes. If we draw such a skeletal graph for the P surface we can easily see (Figure 4) that indeed the networks are identical. One can be moved onto the other by a $[\pm 1/2, \pm 1/2, \pm 1/2]$ translation along any diagonal of the unit cell. The system of networks can be also visualized by the interface surfaces. An example of the parallel surfaces (PS) for the D—double diamond—TPMS based cubic phase is given in Figure 5. The minority block can be contained in the channel bound by a PS defined by

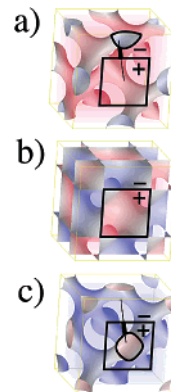


Figure 5. D TPMS (b) shown dividing the volume into two systems of channels. One of them is assigned with the negative values of the displacement ξ and the other with positive ones (blue and red, respectively). This provides a distinction between networks bounded by the parallels surfaces given either by negative displacement (a) or a positive one (c). If an asymmetrical AB diblock copolymer system adopts this geometry the minority block can reside either in the *blue* channel (as drawn in part a) or in the *red* one (c). For balanced TPMS based phases this two situations are identical which is not the case for the unbalanced templates (see Figure 7 for comparison).

either a negative displacement from the base minimal surface (Figure 5a) or by a positive one (Figure 5c). Here the translation needed to move one of the networks onto the other is $\pm 1/2$ in any given direction x , y , or z . Since the networks are identical, the two situations (AB and BA) are indistinguishable and in the analysis of the SAXS patterns it is enough to compute the intensities of the AB structure—the intensities for a BA architecture will be the same. If there is only one interface (an AB architecture) the volume fractions of the channels are $\phi_1^{(A)} = \phi_A$ and $\phi_2^{(B)} = \phi_B$ and $\tilde{\phi}_1 = \phi_1^{(A)} = \phi_A$. The set of $\{I_i^{\text{AB}}\}$ intensities for a monocrystalline sample can be calculated through:

$$I_i^{\text{AB}} = \sum_{hkl: q_{hkl} = q_i} A(\mathbf{q}_{hkl}, \xi(\tilde{\phi}_1)) A^*(\mathbf{q}_{hkl}, \xi(\tilde{\phi}_1)) \quad (2)$$

and for a powder spectrum;

$$I_i^{\text{AB}} = \sum_{hkl: q_{hkl} = q_i} \mathcal{M}_{hkl} A(\mathbf{q}_{hkl}, \xi(\tilde{\phi}_1)) A^*(\mathbf{q}_{hkl}, \xi(\tilde{\phi}_1)) \quad (3)$$

where

$$A(\mathbf{q}_{hkl}, I(\tilde{\phi}_1)) = \mathcal{F}_{hkl}^S \mathcal{F}_{hkl}^M(\xi^*(\tilde{\phi}_1)) \quad (4)$$

the structure factors (SF) \mathcal{F}_{hkl}^S are given in Tables 2–4 of the preceding article.²⁹ For the reflections allowed by the symmetry of the TPMS the Molecular Factor (MF) can be calculated from

$$\mathcal{F}_{hkl}^M(\xi^*) = \frac{\sin(2\pi\sqrt{h^2 + k^2 + l^2} \alpha_{hkl} \xi^*(\tilde{\phi}_1))}{\sin(2\pi\sqrt{h^2 + k^2 + l^2} \alpha_{hkl})} \quad (5)$$

and for the peaks allowed only by the lower symmetry of the networks:

$$\mathcal{F}_{hkl}^M(\xi^*) = \cos(2\pi\sqrt{h^2 + k^2 + l^2} \alpha_{hkl} \xi^*(\tilde{\phi}_1)) \quad (6)$$

The α correction parameters and the forms of the MFs

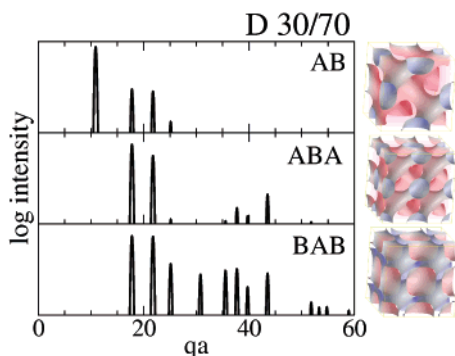


Figure 6. Scattering patterns of three possible cubic architectures in an AB diblock copolymer system adopting geometry of the D-double diamond TPMS. On the right, the corresponding interface parallel surfaces are drawn. The subvolumes occupied by A and B monomers are marked with blue and red, respectively. See text for explanation.

for each of the most prominent reflections of the P, D, and G TPMS based phases are given in Tables 2–4.²⁹

To demonstrate how different are the relative diffraction intensities for the AB, ABA and BAB architectures we have computed the spectra for a double diamond based MCTPS in a diblock copolymer system with the following parameters: $\phi_A = 30$ and $\phi_B = 70$. There are only two different electron densities in the system (ρ_A and ρ_B). Since an arbitrary shift in the overall electron density map does not change the contrast, the electron densities do not enter into equations. Unless $\rho_A = \rho_B$, the difference between them would only change the arbitrary scale on which the intensities are given. The scattering pattern for the AB architecture is shown in the top panel of Figure 6.

For the ABA architecture there are three separate continuous domains of volume fractions equal to $\phi_1^{(A)} = \phi_A/2$, $\phi_2^{(B)} = \phi_B$ and $\phi_3^{(A)} = \phi_A/2$. The volume fractions determining the two interface PSs are $\tilde{\phi}_1 = \phi_1^{(A)} = \phi_A/2$ and $\tilde{\phi}_2 = \phi_1^{(A)} + \phi_2^{(B)} = \phi_A/2 + \phi_B$. The intensities can be calculated through:

$$I_i^{ABA} = \sum_{hkl: q_{hkl}=q_i} \mathcal{M}_{hkl}(\mathcal{F}_{hkl}^S)^2 [\mathcal{F}_{hkl}^M(\xi^*(\tilde{\phi}_1)) - \mathcal{F}_{hkl}^M(\xi^*(\tilde{\phi}_2))]^2 \quad (7)$$

with the MFs calculated through eq 5 or 6 accordingly to their form given in Tables 2–4 of the preceding article. The minus sign in the rectangular bracket comes from the fact that $\tilde{\rho}_1 = \rho_A - \rho_B$ and $\tilde{\rho}_2 = \rho_B - \rho_A = -\tilde{\rho}_1$. The same eq 7 should be used for the BAB architecture with $\tilde{\phi}_1 = \phi_1^{(B)} = \phi_B/2$ and $\tilde{\phi}_2 = \phi_1^{(B)} + \phi_2^{(A)} = \phi_B/2 + \phi_A$. The resulting intensities are contained in Table 1 and two bottom panels of Figure 6. As it is evident from Table 1, the intensities for each of the possible architectures differ significantly enough to be distinguished in a typical scattering experiment.

To compare our results with an experiment and different modeling approach we have computed similar patterns for gyroid architectures in a polystyrene–polyisoprene (SI) diblock system.¹⁴ The third column of Table 2 contains the measured¹⁴ intensities for the composition 0.33/0.67 by volume of the S and I blocks, respectively. The intensities modeled by taking the Fourier Transforms of parallel surfaces¹⁴ are listed in the fourth column. The values in both columns have been divided by a Lorentz–polarization factor for a two-dimensional detector³² for the X-ray wavelength $\lambda = 1.54$

Table 1. Scattering Intensities for the Three Possible Cubic Architectures in an AB Diblock Copolymer System Adopting Geometry of the D-Double Diamond TPMS^a

D 30/70 MCTPS			
$h^2 + k^2 + l^2$	AB	ABA	BAB
3	770	0	0
8	90	567	340
11	3	0	0
12	81	322	328
16	17	12	82
24	8	0	48
32	8	11	58
36	8	22	63
40	2	15	25
43	1	0	0
48	4	45	50

^a The first column contains the squares of the scattering vector spacings. The next three columns give the intensities for the most pronounced peaks in AB, ABA and BAB architectures. For a schematic illustration of the architectures please see Figure 3.

Å and the position of the 211 reflection $q_{211} \approx 0.03 \text{ Å}^{-1}$. This allows us to compare the reported¹⁴ intensities directly to the ones calculated through eqs 3 and 7 for a polystyrene–polyisoprene (SI), polystyrene–polyisoprene–polystyrene (SIS) and ISI gyroid phases, listed in columns 5–7 of Table 2, respectively. The bicontinuous SI structure can be ruled out by the large predicted value of the 110 reflection which was not observed experimentally. Out of the two symmetric, tricontinuous, morphologies the SIS fits the measured intensities better. Significant values of the modeled intensities for the 420 and 332 peaks in the ISI system do not agree with the experimental measurements. For the SIS architecture, both modeling methods (compare columns 4 and 6 of Table 2) yielded similar results. It is worth noting here that the intensities contained in the last three columns can be calculated on a standard spreadsheet software without actual modeling of the interface surfaces.

3.2. Unbalanced Prototypes. The I-WP TPMS is not balanced. It divides the volume of the unit cell into two networks of channels which are not identical. No symmetry operation can move one of the channels onto the other. The channel given by the PS defined by a negative displacement from the base TPMS has four coordinated nodes (Figure 7c) while the one defined by a positive displacement is eight coordinated (Figure 7a). An architecture in which the A blocks are confined within the four coordinated network and the B blocks in the eight coordinated one (AB system) is therefore different from the inverse situation (BA system). Most importantly, any MCTPS architecture based on the I-WP TPMS belongs to the same symmetry group. Thus, it is not possible to distinguish between them by the sole analysis of the peaks spacings. In fact, as it is exemplified below, such an analysis can be misleading.

For the AB architecture $\tilde{\phi}_1 = \phi_A$ (first channel filled with A) and the scattering intensities are given by

$$I_i^{AB} = \sum_{hkl: q_{hkl}=q_i} \mathcal{M}_{hkl}(\mathcal{F}_{hkl}^S)^2 (\mathcal{F}_{hkl}^M(\tilde{\phi}_1))^2 \quad (8)$$

where

$$\mathcal{F}_{hkl}^M(\tilde{\phi}_1) = \cos(2\pi\sqrt{h^2 + k^2 + l^2} \alpha_{hkl}(\xi^*(\tilde{\phi}_1) - \xi_{hkl}^*)) \quad (9)$$

Table 2. Measured and Modeled Scattering Intensities for the Polystyrene–Polyisoprene Diblock System Reported in Ref 14^a

Intensities for the G Polystyrene (S)–Polyisoprene (I) ¹⁴ Diblock Cubic Phases						
hkl	$h^2 + k^2 + l^2$	measd ^a	SIS ^a	SI	SIS	ISI
1 1 0	2	NO	0.000	5.828	0.000	0.000
2 1 1	6	1.000	1.000	1.000	1.000	1.000
2 2 0	8	0.0928	0.224	0.209	0.179	0.210
3 1 0	10	NO	0.000	0.040	0.000	0.000
2 2 2	12	NO	0.000	0.042	0.000	0.000
3 2 1	14	NO	0.005	0.065	0.002	0.033
4 0 0	16	NO	<0.001	0.040	<0.001	0.042
4 2 0	20	0.003	0.003	0.131	0.004	0.141
3 3 2	22	0.007	0.029	0.259	0.015	0.280
4 2 2	24	NO	0.024	0.075	0.014	0.083
431 + 510	26	NO	0.035	0.066	0.019	0.071
5 2 1	30	NO	0.005	0.011	0.004	0.009

^a The third and fourth columns contain the measured and modeled¹⁴ intensities multiplied by the Lorentz–polarization factor. As such they can be compared with the predicted intensities for a bicontinuous polystyrene–polyisoprene (SI) and tricontinuous polystyrene–polyisoprene–polystyrene (SIS) and ISI morphologies calculated through eqs 3 and 7 of this article. NO = not observed. In column 6, we find that SIS architecture calculated by our simple method is in accordance with the experimental results (column 3) and a different simulation method (column 4). The other architectures computed here (SI and ISI) do not agree with the experiment.

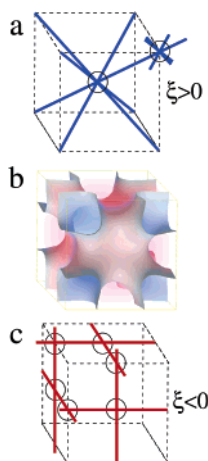


Figure 7. Schematic illustration of the connectivity of the two networks into which the volume is divided by the I-WP TPMS (shown in part b). (a) Skeletal graph of the channels associated with positive displacements ξ and (c) a graph for the four coordinated network associated with negative ξ .

and the $\mathcal{F}_{hkl}^S \propto \alpha_{hkl}$ and ξ_{hkl}^* parameters given in Table 5 of the preceding article.²⁹ For the BA system $\tilde{\phi}_1 = \phi_B$ and the same (eqs 8 and 9) equations should be used. Both scattering intensity diagrams for the AB and BA architecture in a ($\phi_A = 0.3$, $\phi_B = 0.7$) diblock system are presented in the upper panels of Figure 8. The scattering patterns are significantly different. For example in the case of the BA architecture the 200 reflection is absent due to a low value of the MF. An absence of a low-order peak might in general lead to an incorrect determination of the symmetry group of the system. For the ABA MCTPS based on I-WP TPMS the volume fractions defining the two interface PSs are $\tilde{\phi}_1 = \phi_A/2$ and $\tilde{\phi}_2 = \phi_A/2 + \phi_B$. The expression for the intensities reads as follows:

$$I_i^{AB} = \sum_{hkl: q_{hk} = q_i} \mathcal{M}_{hkl} (\mathcal{F}_{hkl}^S)^2 (\mathcal{F}_{hkl}^M(\tilde{\phi}_1) - \mathcal{F}_{hkl}^M(\tilde{\phi}_2))^2 \quad (10)$$

For the BAB architecture $\tilde{\phi}_1 = \phi_B/2$ and $\tilde{\phi}_2 = \phi_B/2 + \phi_A$. The scattering patterns for the ABA and BAB architectures for 30/70I-WP TPMS based MCTPS are shown in the bottom panels of Figure 8. Again the difference in relative intensities for each of the explored architectures

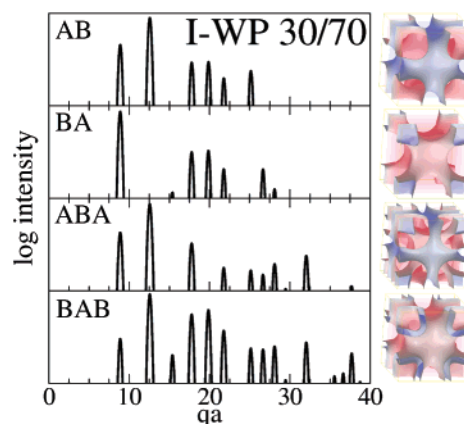


Figure 8. Scattering patterns of the four possible cubic architectures in an AB diblock copolymer system adopting geometry of the I-WP—wrapped package TPMS. The corresponding interface surfaces are drawn on the right to each pattern with the A and B monomer rich subvolumes marked with blue and red, respectively.

gives a reliable data to determine which MCTPS has been formed in the system.

4. Triblock Systems

A triblock copolymer molecule is a linear sequence of blocks A, B, and C. Each of the blocks is composed of the same type of monomers. As far as computing the X-ray scattering intensities goes the main difference to the diblock systems is that now there are three different electron densities ρ_A , ρ_B , and ρ_C in the system. Even though the density map can be shifted by an arbitrary value, now the densities enter the equations.

Analogous to the discussion on the MCTPS phases built from the diblock copolymers, we will take into account four simplest possible architectures. The first is ABC—the A blocks in a channel originating in the negative displacements, B blocks forming a layer around them, and C blocks in a channel filling the volume of the unit cell up to the largest positive values of ξ . An inverse possibility is CBA architecture. The two other possibilities are the symmetrized architectures called ABCBA and CBABC.

4.1. Balanced Prototypes. As in the case of the diblock systems, the two simplest architectures ABC and CBA are identical. For the ABC structure, the

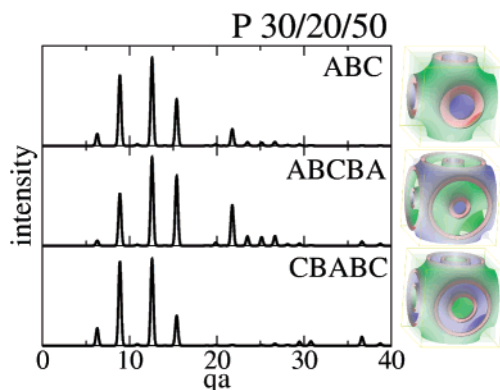


Figure 9. Scattering patterns of the three possible cubic architectures in an ABC triblock copolymer system adopting geometry of the P-plumber's nightmare TPMS. The distinct subvolumes are marked with the different colors: blue (A), red (B), and green (C)

summed volume fractions are $\tilde{\phi}_1 = \phi_A$, $\tilde{\phi}_2 = \phi_A + \phi_B$. The most convenient way is to subtract the electron density of the third block ρ_C from the density distribution. The electron densities used in equations are: $\tilde{\rho}_1 = \rho_A - \rho_B$ and $\tilde{\rho}_2 = \rho_B - \rho_C$. The intensities are calculated as follows:

$$I_i^{ABC} = \sum_{hkl: q_{hkl} = q_i} \mathcal{M}_{hkl} (\mathcal{F}_{hkl}^S)^2 \left[\sum_{j=1}^2 \tilde{\rho}_j \mathcal{F}_{hkl}^M(\tilde{\phi}_j) \right]^2 \quad (11)$$

where the MFs are given by eqs 5 and 6 and their forms together with other parameters can be read from Tables 2–4.²⁹ We have computed the scattering patterns for a P-plumber's nightmare-TPMS based architectures in a following triblock system: volume fractions $\phi_A = 0.3$, $\phi_B = 0.2$, and $\phi_C = 0.5$ and electron densities $\rho_A = 1.0$, $\rho_B = 0.8$, and $\rho_C = 1.2$. The intensities for an ABC architecture are shown in the uppermost panel of Figure 9.

For the ABCBA MCTPS, the summed volume fractions and electron densities used for computations are

$$\tilde{\phi}_1 = \phi_A/2 \quad \tilde{\rho}_1 = \rho_A - \rho_B \quad (12)$$

$$\tilde{\phi}_2 = \phi_A/2 + \phi_B/2 \quad \tilde{\rho}_1 = \rho_B - \rho_C \quad (13)$$

$$\tilde{\phi}_3 = \phi_A/2 + \phi_B/2 + \phi_C \quad \tilde{\rho}_1 = \rho_C - \rho_B \quad (14)$$

$$\tilde{\phi}_4 = \phi_A/2 + \phi_B + \phi_C \quad \tilde{\rho}_1 = \rho_B - \rho_A \quad (15)$$

The index in the innermost sum of eq 11 runs from 1 to 4. For the CBABC structure the volume fractions and electron densities can be recovered from eqs 12–15 by substituting every A with C and C with A. The corresponding diffraction patterns are shown in the middle and bottom panels of Figure 9.

The ABCBA pattern is markedly different from ABC and CBABC. The similarity of the latter two is an example showing that only a detailed quantitative analysis of the intensities of the Bragg reflections together with examination of the lattice parameter and resulting interface areas per copolymer molecule can provide an unambiguous distinction between different possible architectures.

Figure 10 shows the scattering patterns for three possible architectures based on G-gyroid-TPMS formed in an ABC triblock copolymer system of volume fractions $\phi_A = 0.25$, the corresponding electron densities $\rho_A = 1.0$,

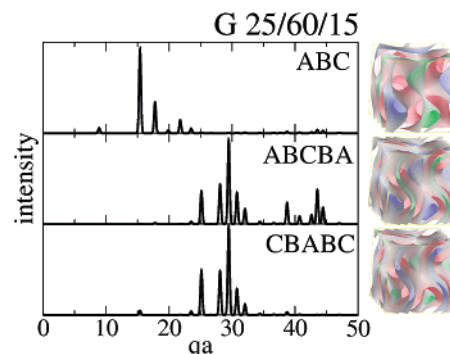


Figure 10. Scattering patterns of the three possible cubic architectures in an ABC triblock copolymer system adopting geometry of the G-gyroid TPMS. The colors are the same as in Figure 9.

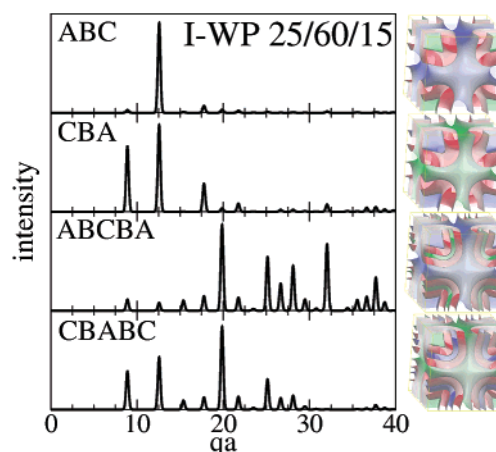


Figure 11. Scattering patterns of the three possible cubic architectures in an ABC triblock copolymer system adopting geometry of the I-WP-wrapped package TPMS. The colors are the same as in Figure 9.

$\rho_B = 0.8$, and $\rho_C = 1.2$. For the ABC architecture, the scattering intensity is concentrated in the low-order Bragg reflections. For the symmetrized architectures ABCBA and CBABC, the MFs of the small hkl index peaks are very weak and the scattering intensity is shifted toward longer scattering vectors. This in principle, especially when the experimental resolution is small, might cause a misdetermination of the lattice parameter a . Comparison of the experimental patterns with modeled intensities should solve this problem.

4.2. Unbalanced Prototypes. As in the case of diblock copolymer systems, the assumption that the MCTPS architecture is based on an unbalanced TPMS requires checking out the two orientations of the copolymer molecule—ABC and CBA. The scattering intensities for the I-WP based structures should be computed with eq 11 and the MF given by eq 9. The calculated intensities are shown in Figure 11. The uppermost panel corresponds to the ABC architecture in which the A block occupy the four coordinated network and the C block are within the eight coordinated one. The pattern for ABC architecture is drastically different from the pattern of an inverse structure CBA. The difference between these two might play a crucial role in materials prepared by selective etching of one or two of the blocks. The ABCBA and CBABC architecture can also be easily confirmed or rejected by comparison with the modeled spectra.

5. Extracting the Interface Width

Let us first discuss a diblock copolymer system for which we have a set of k peaks with the measured scattering intensities $\{I_i^{\text{exp}}\}$. We assume that we have already compared them with the modeled intensities for each of the possible architectures and chosen the set $\{I_i^{\text{mod}}\}$ which yields the best fit. If the choice is correct, they should satisfy the following relation

$$\forall i: I_i^{\text{exp}} = c I_i^{\text{mod}} \exp\left[-\frac{1}{4} q_i^2 \alpha_{hkl}^2 d^2\right] \quad (16)$$

where c is some unknown constant and d is the width of the interface. After taking the natural logarithm of both sides and some rearrangements, we obtain

$$y_i = x_i \ln c + d^2 \quad (17)$$

where

$$y_i = -\frac{4}{\alpha_{hkl}^2 q_i^2} \ln\left(\frac{I_i^{\text{mod}}}{I_i^{\text{exp}}}\right) \quad (18)$$

and

$$x_i = -\frac{4}{\alpha_{hkl}^2 q_i^2} \quad (19)$$

This is a standard statistical problem most easily solved by the means of linear regression which provides:

$$\ln c = \frac{\sum_{i=1}^k x_i \sum_{i=1}^k y_i - k \sum_{i=1}^k x_i y_i}{(\sum_{i=1}^k x_i)^2 - k \sum_{i=1}^k x_i^2} \quad (20)$$

and

$$d^2 = \frac{\sum_{i=1}^k x_i \sum_{i=1}^k x_i y_i - \sum_{i=1}^k y_i \sum_{i=1}^k x_i^2}{(\sum_{i=1}^k x_i)^2 - k \sum_{i=1}^k x_i^2} \quad (21)$$

The standard deviations S of $\ln c$ and d^2 are given by

$$S_{\ln c} = \sqrt{\frac{\frac{k}{k-2} \sum_{i=1}^k \epsilon_i^2}{k \sum_{i=1}^k x_i^2 - (\sum_{i=1}^k x_i)^2}} \quad (22)$$

and

$$S_{d^2} = \sqrt{\frac{\frac{1}{k-2} \sum_{i=1}^k \epsilon_i^2 \sum_{i=1}^k x_i^2}{k \sum_{i=1}^k x_i^2 - (\sum_{i=1}^k x_i)^2}} \quad (23)$$

Table 3. Influence of the Interface Width on the Scattering Intensities from an AB Gyroid Cubic Phase

Intensity for the G 40/60 AB MCTPS				
$(qa/2\pi)^2$	$d^* = 0.0$	$d^* = 0.02$	$d^* = 0.04$	$d^* = 0.1$
2	10000	10000	10000	10000
6	314	307	289	189
8	134	131	122	75
10	91	89	81	43
12	364	351	316	152
14	105	100	87	33
16	70	66	55	15
20	64	60	48	10
22	131	121	96	19
24	42	39	29	4
26	30	27	21	2

^a Each column contains intensities for a different normalized interface width $d^* = d/a$ where a is the lattice parameter.

where

$$\sum_{i=1}^k \epsilon_i^2 = \sum_{i=1}^k y_i^2 - \ln c \sum_{i=1}^k x_i y_i - d^2 \sum_{i=1}^k y_i \quad (24)$$

In the case of triblock or multiblock systems, the analysis is much more complicated. If the interface widths are similar, one can use the latter equations to extract an average interface width. If such an approximation is not justified, one has to use the whole expression for the scattering amplitude (eq 35 of the preceding article²⁹), which makes the statistical analysis more complicated.

As an example, we have computed the scattering intensities for several diblock samples of a different interface width organized in the gyroid AB structure. The results are contained in Table 3.

6. Conclusions and Outlook

The model presented in the preceding paper²⁹ together with the straightforward application methods discussed here should greatly facilitate a reliable determination of the details of multi continuous cubic phases formed in block copolymer systems. As has been shown in sections 3 and 4, it should be possible to either discern or confirm different architecture proposals. The method should allow determination of fine details of the structure as for example whether a given AB diblock system has adopted an I-WP TPMS based structure with the A block in the four coordinated network or in the eight coordinated one. We hope that the detailed description of reconstructing the scattering patterns for various assumed architectures will make the quantitative analysis a standard procedure in the small-angle X-ray and neutron scattering experiments on cubic block copolymer systems.

Acknowledgment. This work has been supported by the Komitet Badań Naukowych Grant 2 P03B00923 (2002-2004) and 5P03B01121. P.G. acknowledges a fellowship from The Foundation For Polish Science.

References and Notes

- (1) Thomas, E. L.; Alward, D. B.; Kinning, D. J.; Martin, D. C.; Handlin, D. L.; Fetters, L. J. *Macromolecules* **1986**, *19*, 2197.
- (2) Hamley, I. W. *The physics of block copolymers*; Oxford University Press: New York, 1998.
- (3) Spontak, R. J.; et al. *Macromolecules* **1996**, *29*, 4494.
- (4) Schulz, M. F.; et al. *Macromolecules* **1996**, *29*, 2857.

- (5) Hanley, K. J.; Lodge, T. P.; Huang, C. I. *Macromolecules* **2000**, *33*, 5918.
- (6) Seki, M.; Suzuki, J.; Matsushita, Y. *J. Appl. Cryst.* **2000**, *33*, 285.
- (7) Wang, C. Y.; Lodge, T. P. *Macromol. Rapid Commun.* **2002**, *23*, 49.
- (8) Ren, Y.; Lodge, T. P.; Hillmyer, M. A. *Macromolecules* **2002**, *35*, 3889.
- (9) Lodge, T. P.; Pudil, B.; Hanley, K. J. *Macromolecules* **2002**, *35*, 4707.
- (10) Babin, V.; Garstecki, P.; Holyst, R. *Phys. Rev. B* **2002**, *66*, 235120.
- (11) Edrington, A. C.; et al. *Adv. Mater.* **2001**, *13*, 421.
- (12) Simon, P. F. W.; Ulrich, R.; Spiess, H. W.; Wiesner, U. *Chem. Mater.* **2001**, *13*, 3464.
- (13) Schulz, M. F.; Bates, F. S.; Almdal, K.; Mortensen, K. *Phys. Rev. Lett.* **1994**, *73*, 86.
- (14) Hajduk, D. A.; Harper, P. E.; Gruner, S. M.; Honeker, C. C.; Kim, G.; Thomas, E. L.; Fetters, L. J. *Macromolecules* **1994**, *27*, 4063.
- (15) Förster, S.; Khandpur, A. K.; Zhao, J.; Bates, F. S.; Hamley, I. W.; Ryan, A. J.; Bras, W. *Macromolecules* **1994**, *27*, 6922.
- (16) Suzuki, J.; Seki, M.; Matsushita, Y. *J. Chem. Phys.* **2000**, *112*, 4862.
- (17) Shefelbine, T. A.; Vigild, M. E.; Matsen, M. W.; Hajduk, D. A.; Hillmyer, M. A.; Cussler, E. L.; Bates, F. S. *J. Am. Chem. Soc.* **1999**, *121*, 8457.
- (18) Finnefrock, A. C.; et al. *Ang. Ch. Int. Ed.* **2001**, *40*, 1207.
- (19) Matsen, M. W. *Phys. Rev. Lett.* **1995**, *74*, 4225.
- (20) Dotera, T. *Phys. Rev. Lett.* **2002**, *89*, 205502.
- (21) Wohlgenuth, M.; Yufa, N.; Hoffman, J.; Thomas, E. L. *Macromolecules* **2001**, *34*, 6083.
- (22) Gózdź, W. T.; Holyst, R. *Phys. Rev. E* **1996**, *54*, 5012.
- (23) Hajduk, D. A.; Harper, P. E.; Gruner, S. M.; Honeker, C. C.; Thomas, E. L.; Fetters, L. J. *Macromolecules* **1995**, *28*, 2570.
- (24) Mogi, Y.; Mori, K.; Matsushita, Y.; Noda, I. *Macromolecules* **1992**, *25*, 5412.
- (25) Matsen, M. W. *J. Chem. Phys.* **1998**, *108*, 785.
- (26) Stadler, R.; Auschra, C.; Beckmann, J.; Krappe, U.; Voigt-Martin, I.; Leibler, L. *Macromolecules* **1995**, *28*, 3080.
- (27) Krappe, U.; Stadler, R.; Voigt-Martin, I. *Macromolecules* **1995**, *28*, 4558.
- (28) Bates, F. S.; Fredrickson, G. H. *Phys. Today* **1999**, *52*, 32.
- (29) Garstecki, P.; Holyst, R. *Macromolecules* **2003**, *36*, 9181.
- (30) There has been a number of successful attempts of modeling the SAXS spectra of multicontinuous cubic phases in block copolymer mixtures as for example: Harper, P. E. Ph.D. Thesis, Princeton University, Princeton, NJ, 1994, refs 14 and 16. The methods presented there require however computationally demanding modeling of the interfaces.
- (31) Garstecki, P.; Holyst, R. *Langmuir* **2002**, *18*, 2519.
- (32) Garstecki, P.; Holyst, R. *Langmuir* **2002**, *18*, 2529.
- (33) Chu, B.; Hsiao, B. S. *Chem. Rev.* **2001**, *101*, 1727.
- (34) One can imagine even more complicated geometries with several A and B domains span within a single unit cell yet there is neither theoretical nor experimental support for their existence.

MA0212590